New isomer found in $^{140}_{51}Sb_{89}$: Sphericity and shell evolution between $N = 82$ and $N = 90$

R. Lozeva,[1,*] H. Naïdja,[1,2,3] F. Nowacki,[1] J. Dudek,[1] A. Odahara,[4] C.-B. Moon,[5] S. Nishimura,[6] P. Doornenbal,[6]
J.-M. Daugas,[7] P.-A. Söderström,[6] T. Sumikama,[8] G. Lorusso,[6] J. Wu,[9,6] Z. Y. Xu,[10] H. Baba,[6] F. Browne,[11,6] R. Daido,[4,6]
Y. Fang,[4,6] T. Isobe,[6] I. Kojouharov,[2] N. Kurz,[2] Z. Patel,[12,6] S. Rice,[12,6] H. Sakurai,[6,10] H. Schaffner,[2] L. Sinclair,[13,6]
H. Watanabe,[14] A. Yagi,[4,6] R. Yokoyama,[15] T. Kubo,[6] N. Inabe,[6] H. Suzuki,[6] N. Fukuda,[6] D. Kameda,[6] H. Takeda,[6] D. S. Ahn,[6]
D. Murai,[16] F. L. Bello Garrote,[17] F. Didierjean,[1] E. Ideguchi,[18] T. Ishigaki,[4,6] H. S. Jung,[19] T. Komatsubara,[20] Y. K. Kwon,[20]
P. Lee,[21] C. S. Lee,[21] S. Morimoto,[4,6] M. Niikura,[10] H. Nishibata,[4,6] and I. Nishizuka[8,6]

[1]IPHC, CNRS, IN2P3, and University of Strasbourg, F-67037 Strasbourg Cedex 2, France
[2]GSI Helmholtzzentrum für Schwerionenforschung GmbH, D-64291 Darmstadt, Germany
[3]University of Constantine, 25000 Constantine, Algeria
[4]Department of Physics, Osaka University, Osaka 560-0043 Toyonaka, Japan
[5]Department of Display Engineering, Hoseo University, Chung-Nam 336-795, Republic of Korea
[6]RIKEN Nishina Center, Wako-shi, Saitama 351-0198, Japan
[7]CEA, DAM, DIF, F-91297 Arpajon Cedex, France
[8]Department of Physics, Tohoku University, Miyagi 980-8578, Japan
[9]School of Physics and State Key Laboratory of Nuclear Physics and Technology, Peking University, Beijing 100871, China
[10]Department of Physics, University of Tokyo, Tokyo 113-0033, Japan
[11]School of Computing, Engineering and Mathematics, University of Brighton, Brighton BN2 4GJ, United Kingdom
[12]Department of Physics, University of Surrey, Guildford GU2 7XH, United Kingdom
[13]Department of Physics, University of York, Heslington, York YO10 5DD, United Kingdom
[14]School of Physics and Nuclear Energy Engineering, Beihang University, Beijing 100191, China
[15]CNS, University of Tokyo, Wako, Saitama 351-0198, Japan
[16]Department of Physics, Rikkyo University, Toshima, Tokyo 171-8501, Japan
[17]Department of Physics, University of Oslo, N-0316 Oslo, Norway
[18]RCNP, Osaka University, Ibaraki, Osaka 567-0047, Japan
[19]Department of Physics, University of Notre Dame, Notre Dame, Indiana 46556, USA
[20]Rare Isotope Science Project, Institute for Basic Science, Daejeon 305-811, Republic of Korea
[21]Department of Physics, Chung-Ang University, Seoul, Republic of Korea

In this article we report on the first spectroscopic information on $^{140}_{51}Sb_{89}$ and the observation of an isomer in this nucleus with $T_{1/2} = 41(8)$ μs. It is located in close proximity to ^{140}Sn for $N = 90$, where the $\nu f_{7/2}$ orbit is completely filled. The possible origin of the isomeric state is a $\pi g^1_{7/2} \times \nu f^{-1}_{7/2}$ coupling configuration, resulting in a (6^-) or (7^-) spin-parity. This is likely caused by an inversion of the $\pi g_{7/2}$ and $\pi d_{5/2}$ orbitals at $N = 89$. The existence of such an isomer far from stability is discussed extensively in the context of shell-model calculations and compared to results from mean-field calculations performed using a deformed Woods-Saxon potential. Both approaches suggest the observation of a single-particle excitation mode at an extreme neutron number.

I. INTRODUCTION

Many species in the nuclear landscape are still unknown. For example, for nuclei with large N/Z ratios, several questions are apparent as what are the excitation schemes of these nuclei and how strongly are they influenced by the large amount of neutrons. In addition, in neutron-rich nuclei, the $T = 1$ and $T = 0$ channels of the nuclear effective interaction weigh differently than they do closer to the stability line. Therefore, for such systems dramatic shell ordering changes may occur, leading to the vanishing of known shell closures and/or to the occurrence of new magic numbers. This is the case, for example, for the new magic number $N = 34$ in ^{54}Ca [1] or the vanishing of shell closure at $N = 20$ and 40 [2,3] (the reader is referred to Ref. [4] for an extensive review of shell drift mechanisms). Being very exotic, it was suggested that the nucleus is forming a neutron skin [5] which may also evolve [6] with the further addition of nucleons [7] as a result of, e.g., broken proton-neutron exchange symmetry [8].

Especially in the ^{132}Sn region, experimental information about the neutron skin is lacking due to various experimental difficulties, among which is the requirement of a stable target of the nucleus being studied. Measurements of the neutron skin were successfully performed in the next-major shell for ^{208}Pb [9]. If there are similarities between these two major shells, as suggested in Refs. [10,11], the development of a neutron skin may be expected also in the neutron-rich nuclei beyond ^{132}Sn. Indeed, in both regions several analog excitation schemes of isomeric decays were found to exist, e.g., yrast isomers in ^{134}Sb and ^{210}Bi [12–14]; ^{136}Sb and ^{212}Bi [10,11] formed

*radomira.lozeva@iphc.cnrs.fr

on the equivalent $\pi g_{7/2} \nu f_{7/2}$ and $\pi h_{9/2} \nu g_{9/2}$ proton-neutron multiplets.

A link between the variation of the one-particle shell structure and the surface diffuseness of the nuclear potential was already expected for very neutron-rich nuclei far from stability towards the neutron drip line [15]. Mean-field (MF) calculations, using the SKX Skyrme interaction [16], suggested that the changes for the particle-particle and the particle-hole states in very neutron-rich $_{51}$Sb$_{N<94}$ and $_{81}$Tl$_{N<128}$ nuclei are related to the formation of a neutron skin in the heavy isotopes beyond $_{50}$Sn [7,17]. Also, according to shell-model (SM) calculations, the extra neutrons acting as a skin influence the rapid change in the isomeric schemes of the heavy ^{134,136}Sb isotopes [10,11]. It is intriguing to find how these schemes would evolve at more extreme N. For example, it was calculated that the effect on the evolution of the proton single-particle energies of odd-even Sb nuclei [7,18] may be very sudden, because the neutron skin that appears above $N = 82$ surprisingly shall weaken around $N = 90$.

With the increase of the valence neutrons, the nuclei beyond ^{132}Sn may be expected to develop collective properties. Seniority mixing was important in the description of isomers in the ^{134,136,138}Sn nuclei with only few neutrons in the $\nu f_{7/2}$ shell [19,20]. A similar conclusion was given when adding protons to the ^{132}Sn core for, e.g., Sb and Te isotopes [21]. Isomeric half-lives in these nuclei were found to decrease as a result of configuration mixings in ^{133,135}Sb and ^{134}Te [22–24]. Particularly, with the increase of both protons and neutrons, in midshell regions where many-valence-particle excitation modes are present, one may expect transitional properties. Increased configuration mixing of deformed states had to be included in the description of experimental data for, e.g., Te and Xe [25] but also deformation [26] that may cause the formation of complicated shapes [27]. Interestingly, μs isomeric states were observed along the semimagic $Z = 50$ [22,24] and $N = 82$ nuclei [19,28]. However, very few examples were reported beyond these lines [23], despite some theoretical predictions [29]. One may expect that, due to highly mixed wave functions and collectivity, their lifetimes become rather short in the nanosecond or sub-nanosecond region, unless another structural effect prevails the orbital evolution in these very exotic nuclei.

Within the SM framework and empirical interactions an effect of a subshell gap was suggested in Ref. [30] between the $\nu f_{7/2}$ and the $\nu p_{3/2}$ orbitals at $N = 90$. According to an independent Hartree-Fock-Bogoliubov MF calculation within a neutron Cooper-pair transfer formalism in Ref. [31], a structural change may be expected in ^{140}Sn. It could, however, be very localized and have almost equidistant spacing between these $\nu f_{7/2}$ and $\nu p_{3/2}$ orbitals at ^{142}Sn. The proposition of a subshell gap at $N = 90$ was rejected by two follow-up SM works. For example, in Ref. [20] it was shown that the increasing gap $\nu(f_{7/2} - p_{3/2})$ around 2 MeV in ^{140}Sn has an apparent effect on the electromagnetic transitions and the energy levels of the Sn isotopes with $N < 90$. Therefore, this would be inconsistent with recent isomer data [19] and thus the expected shell closure. A similar conclusion was given in Ref. [32] after finding the nearly constant spacing between $\nu(f_{7/2} - p_{3/2})$ when going from ^{134}Sn to ^{140}Sn. It is, therefore,

appealing to find out how the coupling between the predicted magical closure and superfluidity due to pairing interplay with each other at this excessive N and search whether other effects may appear. As ^{140}Sn is itself still difficult to approach experimentally, we studied these competing phenomena in ^{140}Sb, located only one neutron-hole and one proton-particle away.

II. EXPERIMENTAL DETAILS

An isomer and β-decay experiment was performed at the RIBF facility at RIKEN [33] in the framework of the EURICA project [34,35]. It represented a powerful combination of uranium beams with high intensity and a very efficient γ-ray detector system, enabling new detailed spectroscopic studies. An in-flight ^{238}U^{86+} fission at 345 MeV/u was initiated on a ^{9}Be target with a thickness of 2.9 mm. The beam intensity varied between 1 and 5 pnA for the total 4.5 days of measurement time. The nuclei of interest were transported and selected by the BigRIPS and ZeroDegree spectrometers [36]. They were identified using the standard ΔE-ToF-$B\rho$ method and a system of tracking and identification detectors at the focal planes [37]. Offline calibrations and particle tracking were used to achieve unambiguous particle identification [37,38]. The ions were further implanted in the wide-range active stopper for β and ion detection, WAS3ABi. It comprises a stack of five (1-mm-thick) double-sided silicon-strip detectors (DSSSD) with a segmentation of 60×40 strips (1-mm pitch) [34,35].

For the nuclei produced in an isomeric state, with lifetimes long enough to survive in-flight decay through the spectrometers (of the order of 600 ns), delayed γ rays were observed after their implantation. The implantation itself was adjusted with the help of a degrader with variable thickness, used at the final focal plane. Rejection of light particles was assured by veto plastics in front of and behind the setup. The γ rays were detected using the EURICA (4π) array surrounding the stopper (in a close-packed geometry). It was assembled out of 12 Ge cluster detectors (of seven high-purity germanium crystals from the former EUROBALL array [39]) and 18 LaBr$_3$(Ce) detectors [40]. Ion-γ coincidences (for isomeric or β-decay studies) were acquired for different time windows after the implantation using either standard time-to-digital converters for short-time (μs) ranges or digital-gamma-finders for longer-time (tens of μs) ranges. Off-beam, prompt and very long activities could thus be distinguished and used in the background analysis of short or intermediately-long isomeric decays.

III. EXPERIMENTAL OBSERVATIONS AND LEVEL SCHEME

Among all selected products in this experiment we unambiguously identified five Sb isotopes. For the most exotic, ^{140}Sb, we detected about 9.3×10^3 ions, well separated from the rest, about 1×10^7 ions in total [38]. The delayed γ-ray spectrum (after a background subtraction) in coincidence with ^{140}Sb is shown in Fig. 1(a). This is the first spectroscopic data on this nucleus and the experimental spectrum contains two new transitions of 70.9(8) and 227.3(5) keV. They are in
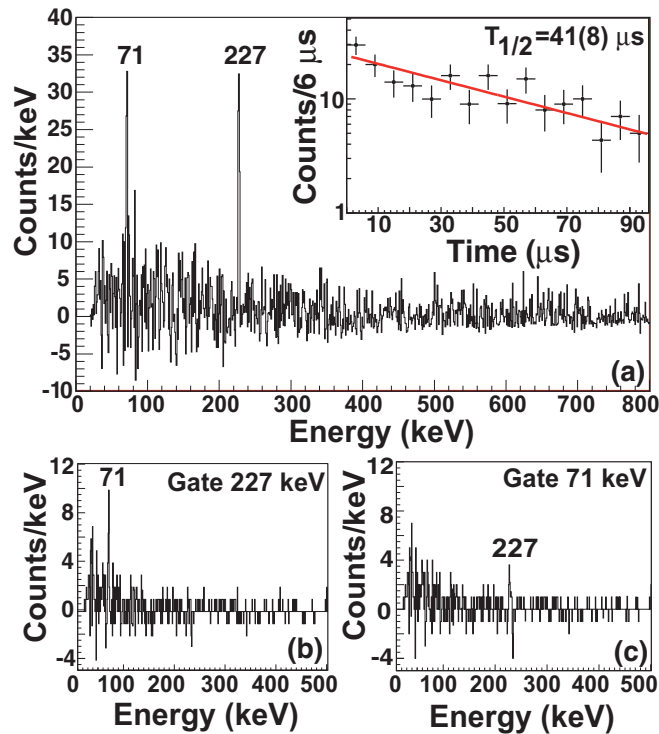
FIG. 1. The delayed and background-subtracted γ-ray spectrum for ^{140}Sb (a). Lifetime fit is shown in the inset and coincidence-gate spectra on each of the transitions are plotted in panels (b) and (c).

mutual coincidence as presented in Figs. 1(b) and 1(c) (for the gates associated with 227.3- and 70.9-keV lines, respectively). Moreover, both transitions have the same lifetime and indicate the existence of an isomeric decay in ^{140}Sb. To improve the statistics, we constructed a background-subtracted sum time spectrum for the 70.9(8)- and 227.3(5)-keV γ rays, shown in the inset of Fig. 1(a). The extracted half-life amounts to $T_{1/2} = 41(8)$ μs.

A simple decay scheme can be constructed using the new spectroscopic information, associating the two transitions in a cascade. The experimental ratio between these transitions, $I_{\gamma 71}/I_{\gamma 227}$, amounts to 1.03(31), taking into account addback, efficiency corrections, and various background subtractions. Further, we use theoretical conversion coefficients from Ref. [41] to find out their order in the level scheme. Lifetime estimates for these transitions show that the 70.9-keV line may be in the μs order, if considered as an $E2$ isomeric transition. However, taking into account the total internal conversion ($\alpha_{\mathrm{TOT}} > 5$ [41]), its intensity is too strong for $E2$ multipolarity as a factor of about 5 would be expected between the two transitions. This is independent of whether the 227.3-keV line is considered with the $M1$ or $E2$ multipolarity (due to a very small $\alpha_{\mathrm{TOT}} < 0.1$ [41]). Note that the $M3$ multipolarity (for any of the abovementioned transitions) would result in a state with a lifetime of seconds, which is not the case and excludes the scenario. Therefore, the experimental observations are consistent with an $M1$ type for the 70.9-keV transition, while for the 227.3-keV line both $M1$ and $E2$ types are possible. Using the respective conversions, the 70.9-keV transition

appears stronger and can then be placed at the bottom of the cascade (see Fig. 2). One may note that the loss in the isomer intensity due to the flight time in the spectrometers is negligible with respect to its lifetime.

For the direct depopulation of the isomer, one can also consider the 227.3-keV line. However, as an $M1$ type, the transition would be far off the experimental lifetime, while an $E2$ type would result in a very small $B(E2)$ value of about 0.02 e^2 fm^4 ($\sim 10^{-4}$ W.u.). Therefore, in such a case, the line would be compatible with the measured lifetime only as a hindered transition. Then, the appearance of the spin ($J + 2$) difference in the populated levels would result in the observation of a spin-trap isomer, which is consistent with a yrast picture. Using the available experimental information we calculated the isomeric ratio for this new isomer and obtained 9(5)%, which is at least five times weaker with respect to the yrast isomer in ^{136}Sb [42].

We therefore conclude that we observed a cascade following an isomeric decay and that it is placed below the isomeric transition. This transition would then be with an energy below our observational threshold. Assuming an $E2$ type, energy below 30 keV would be required, therefore the γ ray will be highly converted ($\alpha_{\mathrm{TOT}} > 100$ [41]). A (nonretarded) transition with $B(E2)$ of about 1 W.u. is typical for this region of nuclei [43], e.g., between states with the same or no deformation and could be considered as a good candidate for the isomeric transition. An alternative to this scenario would be the appearance of an isomeric $M1$ transition of the order of 1–2 keV, as a result of closely overlapping levels. A $B(M1)$ value of the order of 10^{-4} W.u. would then be expected with respect to the experimental lifetime (in comparison to typical values of about 10^{-3} W.u. from systematics in the ^{132}Sn region [43]). In this situation one may also consider the possible l-forbidden $M1$ transitions appearing in such nondeformed nuclei [44]. Therefore, to construct the level scheme, a cascade of three transitions is taken into account. We note that we limited the options for the ground-state (g.s.) spin-parity of
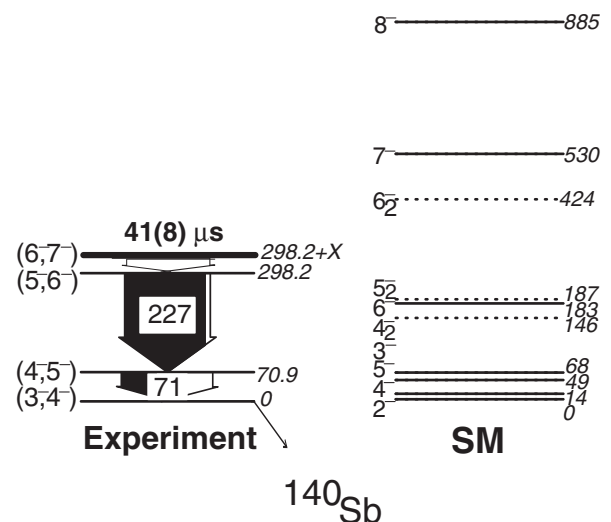

FIG. 2. Experimental level scheme of the observed isomer in ^{140}Sb compared to the results of SM calculations. Yrast and yrare states are represented by solid and dotted lines, respectively.

^{140}Sb to $(3^-, 4^-)$. According to our β-decay ^{140}Sb $\rightarrow ^{140}$Te analysis (subject to another article, Ref. [45]), the g.s. of ^{140}Sb seems to most probably be (4^-). However, the (3^-) alternative cannot be completely excluded from the intensity analysis of the daughter due to a close overlap of transitions populating its respective 4^+ and 2^+ states.

The proposed experimental scheme is presented in Fig. 2, where several possible options for spin-parity of the levels are predicted. The I excited state with a possible spin-parity of (4^-) or (5^-) shall be connected to the g.s. by the 70.9-keV transition. The next excited level, spaced by 227.3 keV, shall most probably have a spin-parity of (5^-) or (6^-). As the isomeric transition is unobserved in this work, we place the isomeric level at the maximum level-energy distance of about 30 keV, while for its spin-parity we propose $(6^-, 7^-)$.

IV. SHELL-MODEL CALCULATIONS

To understand the appearance of this isomer and its decay scheme, we performed SM calculations. For the description, the ^{132}Sn nucleus was used as a core. Valence neutrons were set to occupy the $f_{7/2}, h_{9/2}, f_{5/2}, p_{3/2}, p_{1/2}, i_{13/2}$ model space, while the valence protons were set to occupy the $g_{7/2}, d_{5/2}, d_{3/2}, s_{1/2}, h_{11/2}$ orbitals. The Kuo-Herling effective interaction [46] in a modified version (denoted KH-modified) was employed. The modifications were carried out on the multipole and on the monopole parts. In the multipole part, the diagonal and off-diagonal $f_{7/2}$ pairing matrix elements were increased to obtain the electromagnetic transitions of the ^{134,136,138}Sn isotopes from Refs. [19,28]. The monopole correction to the $\nu f_{7/2} - \pi g_{7/2}$ matrix elements was also increased to obtain the systematic energy levels of neutron-rich odd-mass Sb isotopes reported in Ref. [7], and in particular the g.s. of ^{139}Sb was assumed to be with a spin-parity of $(7/2^+)$ [47]. The SM results are compared to the experimental results in Fig. 2, where the yrast (I excited) multiplet of states up to 7^- is plotted. In addition, the calculated 8^- state of a predominantly $\pi g_{7/2} \nu f_{7/2}^6 h_{9/2}$ origin is shown for comparison, although far off the experimental energies and transition rates. We note that, as theoretically positive-parity states are expected beyond 2 MeV, we do not consider their appearance in our

level scheme. We, therefore, neglect the presence of any $E1$, $E3$, and $M2$ type transitions that may take place between positive- and negative-parity states. In the level scheme, we show also several yrare (II excited) states that are calculated to be in the experimental energy range. These could also be potential candidates for the isomer or states populated in its decay, though they are expected to have the same configuration as the nearby yrast states. To demonstrate this, we refer to Figs. 3(a)–3(c), where we show, respectively, the calculated $B(E2)$ and $B(M1)$ transition rates and the most relevant ν and π configurations for all of these (I and II excited) states.

According to the calculations, none of the predicted sequences of excited states has a yrast spin trap in this nucleus, in contrast to the lighter Sb nuclei [11,42]. From the calculated I excited states, the first 6^- candidate lies closest to the experimental energy. Compared to experiment, the energy spacing of the lower-lying states correlates reasonably well with the order of the experimental transitions. The first 4^- and 2^- states appear as traps and are candidates for the g.s. The predicted 2^- state is lowest in energy, closely followed by a 4^- state (see Fig. 2). Experimentally, this sequence (with a distance of <25 keV) would result in a lifetime of microseconds for the 4^- state, which was not observed, while a lifetime of milliseconds could be formed only with exceptionally small $B(E2)$ of <0.1 e^2 fm^4 [in variance to the predicted values in Fig. 3(a)]. In that case, the 2^- g.s. cannot be populated because the β decay out of the 4^- state would always be preferred. A similar scenario would not be feasible for a I excited 3^- state because the resulting energy difference to the predicted 2^- state would be <0.01 keV.

As this relates to an expected analogy with nuclei from the next major shell, one may note that nonyrast states like the first 0^- state may theoretically be expected at an excitation energy similar to that of the first 6^- state and is predicted with the same configuration. However, no change in its transition [e.g., $B(E2)$] strength can be expected in contrast to the drop predicted for the first 6^- and 7^- yrast states [see Fig. 3(a) and Sec. VI]. Also, no potential decay to the predicted (as g.s.) 2^- state will be consistent with the experimentally observed energies. The appearance of a 0^- state in ^{140}Sb would make a resemblance (similarly to the lighter Sb) to the excitation
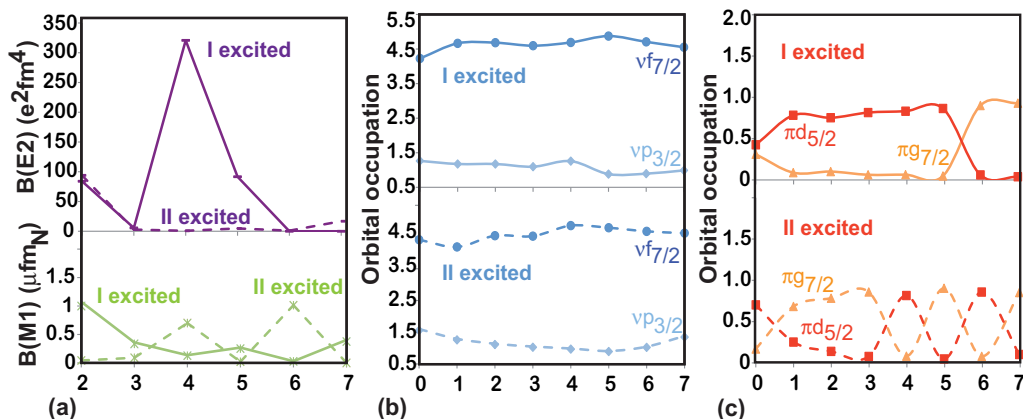

FIG. 3. Theoretical $B(E2; j \rightarrow j - 2)$ and $B(M1; j \rightarrow j - 1)$ transition rates according to the SM (a), most relevant ν orbital occupations (b), and most relevant π orbital occupations (c) for the first (I) excited and second (II) excited states in ^{140}Sb.

schemes in the next-major shell for the Bi chain (e.g., $^{216,8}\text{Bi}$) where high-spin g.s. (6^--9^-) and low-spin isomers [48–50] were suggested. In this case, however, a correlation of that kind could not be made.

V. MEAN-FIELD CALCULATIONS

In addition to the SM, also calculations in the MF approach were employed in this work using the analysis of single (or multiple) particle-hole excitations [51]. The model calculations were performed using a deformed nuclear MF phenomenological Hamiltonian with the Woods-Saxon potential and the universal parameter set. In this implementation time-reversal symmetry was built in the Hamiltonian, and thus time transversal invariance with respect to the positive and negative projections of the total angular momentum. Small and intermediate quadrupole deformations were considered and the solutions were examined using the tilted Fermi surface (TFS) method [51], while separating the occupied from the unoccupied states representing the Fermi energy.

The solution for quadrupole deformation (e.g., $\alpha_{20} = -0.06$) was selected among several calculated cases, because this deformation is representative of small oblate-shape equilibrium deformations in these nuclei. It also takes into account, as a semiquantitative illustration, the single-particle spectrum. This allows at the same time the nuclear systems with nearly filled major gaps to gain (on the average) the minimum excitation energy with maximum alignment of individual nucleonic angular momentum. For ^{140}Sb, the energies obtained for the chosen deformation, minimizing over all possible configurations, are presented in Fig. 4. These results suggest that several local minima of the energy versus spin can be expected, the lowest of which has a spin-parity of (4^-), while other j-shell ν excitations would lead to states of spin-parity of 5^-, 6^-, and 7^- in the close-lying energy range. The (4^-) appears as the best candidate for the g.s., while the other states may be considered as candidates for isomers. Among these, a good candidate with a relative drop with respect to the other states and with an excitation energy close to the experimental
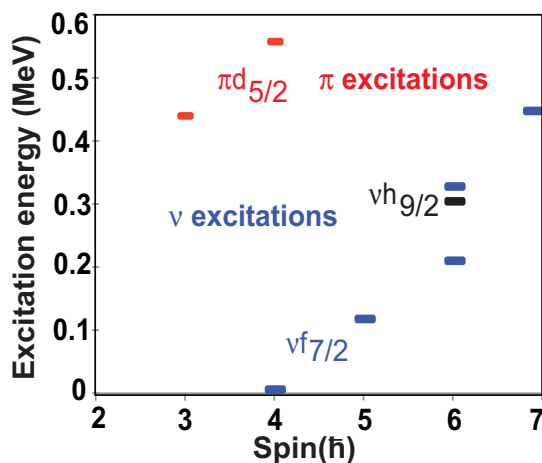
result is 6^-, which is consistent with the SM expectations (see Sec. IV). Observing an isomeric state with a spin-parity of 6^- corresponds to a ν ($j = 3$)-shell excitation, lowered in energy as compared to ($j = 4$)-shell excitations or any π excitations. We note, however, that the relative energies within a given deformed j shell depend on the deformation but very little on a given MF model. Therefore, these energies can be considered more certain. On the other hand, the relative positions of the j shells are strongly spin-orbit, and thus model dependent. The similar remark applies to relative positions of π versus ν levels. This implies, in particular, that the π energies in Fig. 4 are expected to carry stronger uncertainties. An absolute energy difference between the discussed π and ν configurations, within the MF model, cannot be given without minimizing over axial quadruple and hexadecapole deformations, which is not considered here. In addition, the consideration of these deformations will compress the TFS π solutions to lower energies; thus, e.g., the $\pi d_{5/2}$ orbital may become important for the calculated g.s. The current orbital ordering can, therefore, be seen as a semiquantitative guidance. As for this nucleus we have a nearly spherical shape because no collective rotation was observed by manifesting a rotational pattern; the chosen small deformation provides a good overall description in qualitative agreement with the experimental data.

VI. DISCUSSION

The $^{140}_{51}\text{Sb}_{89}$ nucleus has one particle in $\pi g^1_{7/2}$ and the $\nu f_{7/2}$ shell is almost filled with only one hole in $\nu f^{-1}_{7/2}$. Exciting them to other orbitals, appears, however, different from the $^{134}_{51}\text{Sb}_{83}$ nucleus, which has one particle in $\pi g^1_{7/2}$ and one particle in $\nu f^1_{7/2}$ outside the ^{132}Sn core. The reasons for this would be on one hand the Pandya transformation (ph transformation of the $\pi\nu$ interaction) and on the other hand the eventual mixing with other configurations at the end of the shell.

Therefore, two scenarios can cause the newly observed isomeric state.

(i) Close-lying states may result in the appearance of a low-energy $E2$ or $M1$ transition, which is consistent with the long lifetime; thus one can search for these candidates. The spin difference shows that the origin of the isomeric transition may involve both yrast and yrare states. These states are certainly very different from the first multiplet of states {0–7} in the lighter Sb isotopes [14,42]. For the sequence in Fig. 2, this scenario may produce 4^-_2 to 6^-_2 states, predicted around the 6^-_1 state.

(ii) Configurational change for a particular state may also cause the isomerism. This would be plausible with the wave functions of both the 6^-_1 and the 7^-_1 states, making them candidates for the isomer. The $B(E2)$ transition rates calculated by the SM [shown in Fig. 3(a)] suggest a drop for the first 6^- and 7^- states. This indicates that the $B(E2; 7_1 \rightarrow 5_1)$ and $B(E2; 6_1 \rightarrow 4_1)$ values are quite retarded and thus most probably blocked and unobserved. In addition, they are compatible with the respective $B(M1)$ values, also presented in Fig. 3(a),

FIG. 4. Possible spin traps according to the MF, representing the spin and excitation energy of states expected to be occupied in ^{140}Sb.

which makes these $E2$ transitions less probable. Small but not negligible $B(M1)$ rates are expected for the I excited multiplet (with a minimum for the 6_1^- state) and a larger staggering is calculated for the II excited multiplet. This means that, out of an isomeric state with a possible spin-parity of 6^- or 7^-, no retardation is required in the decay to the g.s. Therefore, the isomeric decay can proceed only by a cascade of $M1$ transitions. In comparison with the experimentally expected transition rates for a highly converted low-energy isomeric transition, this scenario would be more coherent with the data.

A closer look at the configurational properties of the calculated states [presented in Figs. 3(b) and 3(c)] reveals the most important $\pi\nu$ orbital excitations, where the weakly present $\nu h_{9/2}$ orbital is omitted (as it is only relevant for states beyond the first 8^-). According to our analysis, the $\nu f_{7/2}$ and $\nu p_{3/2}$ orbitals are populated with equally large strength for all of the states. A difference is found mainly in the π excitations. In particular, the amplitude of the $\pi d_{5/2}$ orbital occupation drops for the 6_1^- state and is replaced by a $\pi g_{7/2}$ strength of about 90%. As can be seen in Fig. 3(c), the same occupation is expected also for the 7_1^- state. The rest of the multiplet members have strong $\pi d_{5/2}$ in their configurations, except the 5_2^- state. The last is, however, not considered as an isomeric candidate following the expectations for transition rates.

Combining the orbital occupation with the excitation energies of the excited states, one can suggest that in energy the $\pi g_{7/2}$ orbital is above the $\pi d_{5/2}$ orbital. Hence, it is most apparent that the isomeric state in the ^{140}Sb nucleus appears due to exactly this change of configuration with respect to the lighter Sb isotopes. This would also be consistent with the wave functions and the excitation energies of the discussed 6_1^- and 7_1^- states and is in agreement with the experimentally suggested spin-parity values.

Two aspects may play a role in this context. On one hand the equidistant spacing between the $\nu f_{7/2}$ and $\nu p_{3/2}$ orbitals [20] has been suggested to provoke a sizable gap [30] at $N = 90$ but this has not been proven experimentally. On the other hand, an effect may be caused by the evolution of the $\pi g_{7/2}$ and $\pi d_{5/2}$ orbitals that may play a role in the formation of a neutron skin. The spacing between them was suggested to drop already at the beginning of the shell for the experimentally observed I excited $5/2^+$ state in ^{135}Sb [7,52] with respect to that in ^{133}Sb [53]. A tendency for a further reduction with the increase of N was suggested in Ref. [7]. One can note, however, that the appearance of non-negligible configuration mixings [21] could also be consistent with the observed behavior.

As presented in Fig. 3(c), the inspection of the calculated wave functions reveals that most of the excited states have a large $\pi d_{5/2}$ orbital occupancy instead of the expected $\pi g_{7/2}$ orbital. Obviously, this is due to the decrease of the proton gap between $\pi g_{7/2}$ and $\pi d_{5/2}$ with filling the $\nu f_{7/2}$ shell. This is illustrated in Table I where the variation of the effective single-particle energy ($\bar{\epsilon}$) splitting between the $\pi g_{7/2}$ and $\pi d_{5/2}$ orbitals between $A = 132$ and $A = 140$ is reported. Due to the relatively more attractive monopole interaction $V_{2f_{7/2}2d_{5/2}}^{pn}$ with respect to the $V_{2f_{7/2}1g_{7/2}}^{pn}$ one, the modified Kuo-Herling

TABLE I. Variation of the effective single-particle energy splitting for the $\pi 1g_{7/2}$ and $\pi 2d_{5/2}$ orbitals between $A = 132$ and $A = 140$ for modified Kuo-Herling, Cd-Bonn, and N3LO effective interactions (see text for details). Their spin-tensor decomposition [54] into central ($K = 0$), spin-orbit ($K = 1$), and tensor ($K = 2$) terms is also given.

$\Delta[\bar{\epsilon}(1g_{7/2}) - \bar{\epsilon}(2d_{5/2})]$	Total	$K = 0$	$K = 1$	$K = 2$
KH-modif	−1.22	−	−	−
CD-Bonn ($10\hbar\omega$)	−1.07	−1.29	−0.49	+0.71
N3LO ($10\hbar\omega$)	−0.96	−1.23	−0.45	+0.72
CD-Bonn ($0\hbar\omega$)	−0.44	−0.84	−0.205	+0.60
N3LO ($0\hbar\omega$)	−0.38	−0.81	−0.17	+0.60

interaction produces a 1-MeV gap reduction with the complete filling of the $\nu f_{7/2}$ shell. This results in a continuous energy decrease of the I excited $5/2^+$ state with N, expected to become g.s. in ^{141}Sb. The microscopic interpretation of this feature can be assessed from the spin-tensor decomposition [54] exposed in Table I for various effective realistic interactions, based on CD-Bonn or chiral effective field theory potentials [55]. The latter two interactions are explicit in the full $0\hbar\omega$ πsdg-νpfh valence space in order to be able to complete the spin-tensor decomposition of the respective effective interactions. The CD-Bonn and the N3LO results correspond to $V_{\mathrm{low}k}$ renormalization with a cutoff of $\Lambda = 2.2$ fm^{-1} in a harmonic oscillator basis with $\hbar\omega = 8.3$ MeV appropriate for $A \sim 112$. Many-body perturbation theory (MBPT) techniques from Ref. [56] are applied respectively in a ten-major-shell basis up to second order to produce CD-Bonn ($10\hbar\omega$) and N3LO ($10\hbar\omega$). The main feature of the spin-tensor analysis is that in all cases the central part is producing the $\pi g_{7/2}$-$\pi d_{5/2}$ gap reduction. This effect is slightly counterbalanced by an opposite tensor behavior. The attractive part of the tensor interaction between the $2f_{7/2}$ ($j_> = l + \frac{1}{2}$) and $1g_{7/2}$ ($j_< = l - \frac{1}{2}$) shells produces a $V_{2f_{7/2}1g_{7/2}}^{pn}$ that is more attractive than the $V_{2f_{7/2}2d_{5/2}}^{pn}$. Finally, the amplitude of the central contribution increases from simple G-matrix or $V_{\mathrm{low}k}$ calculations to full $10\hbar\omega$ MBPT effective interactions. These renormalizations, not included in the original Kuo-Herling effective interaction [46], were therefore incorporated in an ad-hoc phenomenological manner in the modified version used here for the energy spectrum calculations.

One may therefore conclude that the distance between these $\pi g_{7/2}$ and $\pi d_{5/2}$ orbitals is reduced with the increase of N and that $\pi d_{5/2}$ is indeed expected to originate the g.s. in ^{141}Sb. It is thus possible that the orbital crossing appears in ^{140}Sb, which is consistent with the experimental result. Because the influence of the $\pi g_{7/2}$ is present only in excited states due to a close orbital overlap with the $\pi d_{5/2}$, this results in an isomer. The decay then may involve both yrast and yrare states down to the yrast g.s., in agreement with the measured isomeric ratio (see Sec. III). Our conclusion correlates also with the predictions for crossing between these π orbitals at $N = 90$ [57], which we experimentally evidence at $N = 89$.

Furthermore, the ^{140}Sb nucleus has a very small deformation at this extreme neutron number, according to our MF results. Therefore, one may assume that other effects

are playing a role in the formation of its excited states. The difference in the isomeric schemes in ^{136}Sb in comparison to ^{134}Sb, suggested to be caused by the neutron skin [10,11], has certainly evolved in ^{140}Sb. Hence, they may similarly be attributed to the large amount of neutrons, acting as a skin. In fact, an increase of the nuclear radius with N due to development of a neutron skin was expected by the authors of Refs. [7,17]. It appears that it has an influence on the proton single-particle energies of odd-even Sb nuclei, as is indeed proposed in Refs. [7,18]. It is thus possible that this leads to the $\pi g_{7/2}$-$\pi d_{5/2}$ inversion, which we suggest to detect in ^{140}Sb. This effect acts certainly against the expected superfluidity around $N = 90$ [30]. According to both SM and MF calculations presented here, the $\nu f_{7/2}$ and the $\nu p_{3/2}$ orbitals are almost equally occupied for all excited states in ^{140}Sb for $N = 89$, where no changes in their evolution seem to be present. On the other hand, if the effect of a subshell gap is small and very local, one may be able to probe only by a direct-reaction measurement of ^{140}Sn, which is a future experimental challenge.

VII. CONCLUSIONS AND SUMMARY

In this work we observed for the first time spectroscopic information on the very neutron-rich ^{140}Sb nucleus. We found a new isomeric state with a relatively long half-life of $T_{1/2} = 41(8)$ μs. It results from a most-probably single-particle type excitation. Comparing the experimental result to theoretical calculations using the SM and MF frameworks we suggest the $\pi g^1_{7/2} \nu f^{-1}_{7/2}$ configuration for the state, resulting in a most-probable candidate with a spin-parity of (6^-). Furthermore, we

found that the low-energy excitations in ^{140}Sb are influenced not that much by the ν excitations but by the interchanging position of the $\pi d_{5/2}$ and $\pi g_{7/2}$ orbitals.

In addition, we discovered that at the end of the $\nu f_{7/2}$ shell there is a little resemblance with the excitation spectra and the $\pi\nu$ excitations that appear in its beginning and that no magicity seems to be present according to our data. Therefore, the large amount of neutrons may act as a skin that plays a very strong role in the proton excitations (delaying and retarding) or influencing the proton-shell orbital crossing. In this very exotic case, it manifests itself in an isomeric state, possibly due to a change of configuration.

[1] D. Steppenbeck *et al.*, Nature (London) **502** 207 (2013).
[2] C. Thibault *et al.*, Phys. Rev. C **12**, 644 (1975).
[3] O. Sorlin *et al.*, Eur. Phys. J. A **16**, 55 (2003).
[4] O. Sorlin and M.-G. Porquet, Prog. Part. Nucl. Phys. **61**, 602 (2008).
[5] B. A. Brown, Phys. Rev. Lett. **85**, 5296 (2000).
[6] B. A. Brown, A. Derevianko, and V. V. Flambaum, Phys. Rev. C **79**, 035501 (2009).
[7] J. Shergur *et al.*, Phys. Rev. C **65**, 034313 (2002).
[8] D. Bianco, N. Lo Iudice, F. Andreozzi, A. Porrino, and F. Knapp, Phys. Rev. C **88**, 024303 (2013).
[9] S. Abrahamyan *et al.*, Phys. Rev. Lett. **108**, 112502 (2012).
[10] L. Corraggio, A. Covello, A. Gargano, and N. Itaco, Phys. Rev. C **80**, 021305(R) (2009).
[11] A. Covello *et al.*, J. Phys. G: Conf. Ser. **205**, 012004 (2010).
[12] W. Urban *et al.*, Eur. Phys. J. A **5**, 239 (1999).
[13] B. Fornal *et al.*, Phys. Rev. C **63**, 024322 (2001).
[14] J. Shergur *et al.*, Phys. Rev. C **71**, 064321 (2005).
[15] I. Hamamoto *et al.*, Nucl. Phys. A **683**, 255 (2001).
[16] B. A. Brown, Phys. Rev. C **58**, 220 (1998).
[17] P. Sarriguren, M. K. Gaidarov, E. M. de Guerra, and A. N. Antonov, Phys. Rev. C **76**, 044322 (2007).
[18] W. Urban *et al.*, Eur. Phys. J. A **27**, 257 (2006).
[19] G. S. Simpson *et al.*, Phys. Rev. Lett. **113**, 132502 (2014).
[20] H. Naidja *et al.*, J. Phys.: Conf. Ser. **580**, 012030 (2015).

[21] L. Corraggio, A. Covello, A. Gargano, and N. Itaco, Phys. Rev. C **87**, 034309 (2013).
[22] W. Urban, X. Huang, and P. Zhuang, Phys. Rev. C **79**, 034304 (2009).
[23] P. Bhattacharyya *et al.*, Eur. Phys. J. A **3**, 109 (1998).
[24] W. John *et al.*, Phys. Rev. C **2**, 1451 (1970).
[25] J. Äystö, J. Phys.: Conf. Ser. **420**, 012045 (2013).
[26] R. Kshetri, M. S. Sarkar, and S. Sarkar, Phys. Rev. C **74**, 034314 (2006).
[27] W. Urban *et al.*, Phys. Rev. C **62**, 044315 (2000).
[28] A. Korgul *et al.*, Eur. Phys. J. A **7**, 167 (2000).
[29] A. Korgul *et al.*, Eur. Phys. J. A **12**, 129 (2001).
[30] S. Sarkar and M. S. Sarkar, Phys. Rev. C **81**, 064328 (2010).
[31] H. Shimoyama and M. Matsuo, Phys. Rev. C **88**, 054308 (2013).
[32] A. Covello *et al.*, J. Phys.: Conf. Ser. **267**, 012019 (2011).
[33] T. Ohnishi *et al.*, J. Phys. Soc. Jpn. **79**, 073201 (2010).
[34] S. Nishimura, Prog. Theor. Exp. Phys. **2012**, 03C006 (2012).
[35] P.-A. Söderström *et al.*, Nucl. Instrum. Methods Phys. Res., Sect. B **317**, 649 (2013).
[36] T. Kubo *et al.*, Prog. Theor. Exp. Phys. **2012**, 03C003 (2012).
[37] N. Fukuda *et al.*, Nucl. Instrum. Methods Phys. Res., Sect. B **317**, 323 (2013).
[38] R. Lozeva *et al.*, RIKEN Accel. Prog. Rep. **47**, 4 (2014).
[39] J. Eberth *et al.*, Nucl. Instrum. Methods Phys. Res., Sect. A **369**, 135 (1996).
[40] P. H. Regan *et al.*, Eur. Phys. J. **63**, 01008 (2013).

[41] T. Kibèdi *et al.*, Nucl. Instrum. Methods Phys. Res., Sect. A **589**, 202 (2008).
[42] R. Lozeva *et al.*, Phys. Rev. C **92**, 024304 (2015).
[43] www.nndc.bnl.gov, accessed 2015-07-01.
[44] R. Sorensen *et al.*, Phys. Rev. **132**, 2270 (1963).
[45] P. Lee *et al.* (unpublished).
[46] W. T. Chou and E. K. Warburton, Phys. Rev. C **45**, 1720 (1992).
[47] R. Lozeva *et al.* (unpublished).
[48] J. Kurpeta *et al.*, Eur. Phys. J. A **7**, 49 (2000).
[49] E. Ruchowska *et al.*, J. Phys. G: Nucl. Part. Phys. **16**, 255 (1990).
[50] H. De Witte *et al.*, Phys. Rev. C **69**, 044305 (2004).

[51] M. J. A. D. Voigt *et al.*, Rev. Mod. Phys. **55**, 949 (1983).
[52] A. Korgul, H. Mach, B. Fogelberg, W. Urban, W. Kurcewicz, and V. I. Isakov, Phys. Rev. C **64**, 021302(R) (2001).
[53] J. Blomquist, A. Kerek, and B. Fogelberg, Z. Phys. A **314**, 199 (1983).
[54] N. Smirnova *et al.*, Phys. Lett. B **686**, 109 (2010).
[55] D. R. Entem and R. Machleidt, Phys. Rev. C **68**, 041001 (2003).
[56] M. Hjorth-Jensen *et al.*, Phys. Rep. **261**, 125 (1995).
[57] M.-G. Porquet, S. Péru, and M. Girod, Eur. Phys. J. A **25**, 319 (2005).